NAIC-ID(RS)T-0577-94

NATIONAL AIR INTELLIGENCE CENTER

DOUBLET FREQUENCY-BAND TELLURIUM DIOXIDE SOUND-LIGHT OPTICAL DEFLECTOR

by

Binhwa Shu, Haijun Shi, et al.

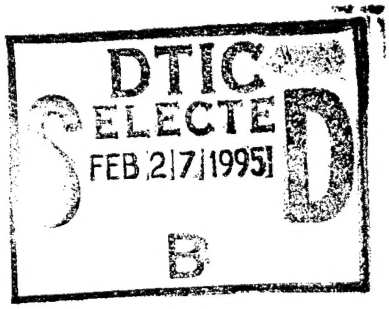

GRAPHICS DISCLAIMER

All figures, graphics, tables, equations, etc. merged into this translation were extracted from the best quality copy available.

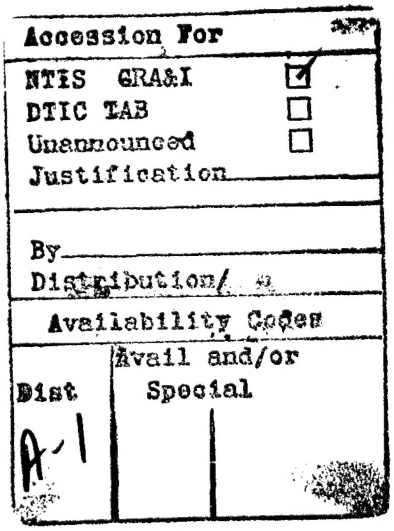

研究报告
Research Reports

Doublet Frequency-band Tellurium Dioxide Sound-Light Optical Deflector

Binhwa Shu, Haijun Shi,
Chihue Zhin and Kwoxen
(Chinese Central Institute,
Shanghai Silicon Oxide Salts
Research Center)
Received on September 30, 1991

This paper proposes that by use of the double-refractive capability of a TeO_2 crystal, one can work out inside a TeO_2 crystal 2 polarization regions, which satisfy the Dixon Equation as its positive and negative solution. In designing instruments, one can make the high-end of the frequency of the No. 1 group exactly contact the low-end of the frequency of the No. 2 group so that the frequency band can be effectively broadened. The ranges of the No. 1 group and No. 2 group used in our study were, respectively, 40 - 80 MHz and 80 - 140 MHz and thus the band-width of the deflector would be 100 MHz.

This paper also proposes a new type of construction for the electric terminals of sonic-optic transducers, to improve the acoustic attenuation, induced by the scatter-spreading processes of the "sound wave modified by truncation" which has to go through such processes in the acoustic field during its propagation inside the TeO_2 crystal.

1. INTRODUCTION

Since the appearance of the tellurium dioxide single crystal [1], it has exhibited excellent acoustic-optic characteristics. Especially, in the propagation along the axial direction of [110], because the vibrating "wave modified by truncation" along the [110] axial direction has a very slow sound speed, one can shorten the sonic-optic

interacting length and at the same time can realize a large deflectional angle, and because of the advantages of having a high point-resolution capability and others, R. W. Dixon [2] and E. G. H. Lea [3], et al, initiated the utilization of direct truncation to study the phase-matching for the "within-the-axis" type of TeO_2 crystalline sonic-optic deflectors. However, in such devices, because it has a modified single switch in the middle frequency range, the "dip" response appears [4]. In 1975, Yano, et al., suggested the TeO_2 deflectors with an asymmetric truncation direction [5]; that is, one can choose any appropriate intersectional angle between the propagation direction of the wave-vector of the "wave modified by truncation" and the [110] axis so that one can move the "dip" region out of the active band-width of the deflector, and thus a sound wave of smoother frequencies can be realized. This kind of devices is commonly called deflectors of the "biased axis type", and their central frequency is intimately related to the crystalline axes of the TeO_2 crystal. If one increases the intersectional angle Θ_a between the propagation direction of the sound wave-vector and the [110] axis, the central frequency of the deflector is also being elevated, and thus its relative band-width becomes broader. However, Θ_a cannot be too large. If Θ_a is taken to be excessively large, the sound speed of the "wave modified by truncation" increases, causing the sonic-optic quality-value M_2 to go down and that in turn increases the intersectional angle between the direction of the sound phase-velocity and the direction of the energy flow; consequently, one will have a disadvantage of needing a larger geometrical size for the TeO_2 crystals.

We made a study on the deflectors whose $\Theta_a = 8°$ and whose band-width could reach 60 MHz. however, at present for any communication processing system, one needs even broader band-widths for the deflectors. Just to increase Θ_a

is not going to work, and thus we started to study TeO_2 deflectors of doublet frequency-band, whose frequency width can reach 100 MHz.

2. PRINCIPLES OF WORKING MECHANISM OF THE INSTRUMENTS

The acoustic properties of a crystalline body can be completely determined by the k-curvilinear surface or the k/Q curvilinear surface $\left(\frac{k}{Q}=\frac{1}{\Lambda f}=\frac{1}{v}\right)$, $\frac{k}{Q}$ and, the k/Q surface in a crystalline body is optically similar to the refractive index curvilinear surface. In general, because a sound wave is neither exactly a longitudinal wave nor a "wave modified by truncation", but the intersectional angle between its vibrational direction and the phase speed direction can be arbitrary. For a uniaxial crystal, if optical rotation can be neglected, the refractive index curve is usually an ellipsoid, but the k/Q curve can be very complex. However, for a TeO_2 deflector, because one only considers the plane formed by the [001] axis and [110] axis, the k/Q curve is still an ellipsoid, whose equation is as follows:

$$\frac{\left[\frac{1}{V_{(\theta_a)}}\right]^2\cdot\cos^2\vartheta_a}{\left[\frac{1}{V_{[110]}}\right]^2}+\frac{\left[\frac{1}{V_{(\theta_a)}}\right]^2\cdot\sin^2\vartheta_a}{\left[\frac{1}{V_{[001]}}\right]^2}=1 \qquad (1)$$

and thus it is not difficult to obtain (illegible)

$$V^2_{(\theta_a)}=V^2_{[110]}\cos^2\theta_a+V^2_{[001]}\sin^2\theta_a. \qquad (2)$$

where Θ_a is the deviation angle of the wave-vector with respect to the [110] axis. In a TeO_2 crystal, the directions of phase velocity and the energy flow of a sound wave are not identical, the intersectional angle Θ_B is as follows:

$$\operatorname{tg}\theta_B=\frac{V^2_{[001]}-V^2_{[110]}}{2V^2_{(\theta_a)}}\sin 2\theta_a \qquad (3)$$

From the initial values of $V_{[110]} = 616\mu m/\mu s$, $V_{[001]} = 2104$ $\mu m/\mu s$, one can calculate, for various axial deviation angles Θa, the supersonic phase velocity $V(\Theta a)$ and the intersectional angle Θ_B between supersonic sound phase velocity V and the energy flow velocity; the results are shown in Table 1.

For a sonic-optical deflector, important parameters are really the band-width, resolution power, and diffraction efficiency. However, for different applications, one needs all different sets of these 3 parameters. For instance, for some high resolution electric frequency-emitting spectrometer, one needs higher frequency resolution power, a radar signal processing system needs a broad diffraction band-width; an electric station detector for jumping frequencies needs high resolution (10 - 20 kHz) as well as broad band-width. At present the band-width available for TeO_2-transverse wave devices in the world is generally 40 - 50 MHz. Table 2 is to show the important functions of the 3 kinds of instruments developed and built by us. From the table, one can see that as Θ_a increases, the band-width broadens, but any further increase in Θ_a becomes impractical. This is due to the fact that as Θ_a increases, $V(\Theta_a)$ also increases and thus it leads to the drops in both resolution (for the given aperture) and the M_2-value. For $\Theta_a = 6°$, M_2 drops off by 16 %, while for $\Theta_a = 8°$, it drops off by 25 % (which corresponds to $\Theta_a = 0$). On the other hand, as Θ_a rises, the intersectional angle between the energy flow direction and the phase-velocity direction becomes larger, and thus one needs a larger crystalline size.

TABLE 1 $V_{\Theta a}$ AND Θ_B FOR VARIOUS Θ_a

θ_a	0	1	2	3	4	5	6	7	8
$v\theta_a$(μm/μs)	616	617	620	625	632	640	651	663	677
θ_B(°)	0	10.6	20.5	28.5	35.2	40.6	44.8	48.1	50.6

Table 2 Essential functions of the 3 kinds of instruments

θ_a (°)	6	7	8
(1) 中心频率 (MHz)	67	78	93
(2) 衍射效率(%)	80	70	60
(3) 带宽 (3dB)(MHz)	40	50	60

Key: (1) central frequency (2) diffraction efficiency (%)
(3) Band-width (3 dB) (MHz)

After we have analyzed the above situations, we concluded that to improve the band-width of the deflectors we had to design a doublet frequency-band TeO_2 sonic-optical deflector. The basic idea of design is to work out the 2 deflectional regions of the Dixon equation within one piece of TeO_2 crystal.

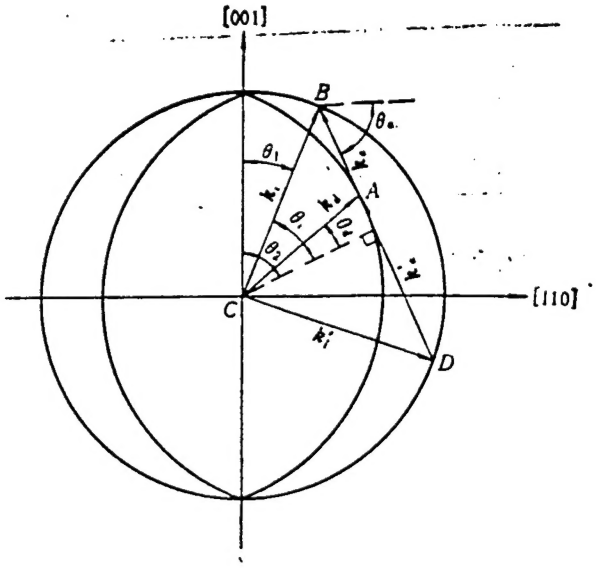

Fig. 1 The wave-vector diagram of a TeO_2 crystal

Fig. 1 shows the diagram of wave-vectors of sonic-optical interaction in a regular uniaxial TeO_2 crystal. In it, k i and ki' stand for, respectively, the incident wave-vectors from 2 different in-coming directions, and kd stands for the wave-vector of the diffraction beam, while ka and ka' stands for, respectively, the acoustic wave-vectors. In order to come up with a broader phase-matching, the "direct truncation phase-matching" is being adopted. As it can be seen from the wave-vector diagram, for each sonic propagation direction, there are 2 closing triangles, ΔABC and ΔADC, both of which satisfy the "direct truncation phase-matching". In other words, for one sonic propagation direction the incident optic beam-fluxes from 2 different directions produce 2 sonic-optic interacting regions of different central frequencies. From the figure, one can see that

$$\begin{cases} k_i = k_d \pm k_a \\ V_i = V_d \pm f_a \end{cases} \tag{4}$$

where V_i stands for the frequency of the incident optical ray, V_d is the frequency of the diffraction ray and f_a is the sound wave frequency. "+-" is determined by the relative position between the incident optical ray and the sound propagational direction, and thus by use of the sine theorems [6], one gets

$$\sin \pm(\theta_a - \theta_1) = \frac{\lambda}{2n_0 V_{(\theta_a)}} \left\{ f + \frac{n_0^2 V_{(\theta_a)}^2}{\lambda^2 f} \times \left[4\delta + \frac{n_e^2 - n_0^2}{n_e^2} \sin^2\theta_1 \right] \right\} \tag{5}$$

$$\sin \pm(\theta_1 - \theta_a) = \frac{\lambda}{2n_0 V_{(\theta_a)}} \left\{ f - \frac{n_0^2 V_{(\theta_a)}^2}{\lambda^2 f} \times \left[4\delta + \frac{n_e^2 - n_0^2}{n_e^2} \sin^2\theta_1 \right] \right\} \tag{6}$$

$$\begin{cases} \theta_i = \pm(\theta_a - \theta_1) \\ \theta_d = \pm(\theta_1 - \theta_a) \end{cases} \tag{7}$$

$$\delta = \frac{\lambda}{360 n_0} \rho \tag{8}$$

where n_o is the ordinary refractive index, n_e is the extraordinary refractive index, and Θ_i and Θ_d are respectively the incident and diffractive angle, while ρ is the optical rotation rate, and Θ_1 and Θ_2 are respectively the intersectional angles of k_i and k_d with respect to the optic axis. From the extreme value condition of Eqn.(6), namely $d\Theta/df = 0$, one finds the extreme value rate f_o to be

$$f_0 = \frac{n_0 V_{(\theta_a)}}{\lambda} \left[4\delta + \frac{n_e^2 - n_0^2}{n_e^2} \sin^2\vartheta_1 \right]^{1/2} \tag{9}$$

By finding the numerical solutions of Eqns. (5), (6), and (9), one gets the 2 sets of corresponding solutions of triangles, ΔABC and ΔADC, and the results are listed in Table 3.

Table 3 The relationships between Θ_a and f_o, as well as Θ_i and Θ_d

θ_s(°)		0	1	2	3	4	5	6	7	8
sin+	θ_i(°)	−1.01	0.06	0.99	1.86	2.68	3.47	4.24	5.01	5.78
	f_s(MHz)	38.06	38.04	40.55	41.54	52.25	61.19	71.25	82.12	93.87
sin−	θ_i(°)	1.01	2.22	3.56	4.98	6.44	7.92	9.41	10.91	12.01
	f_s(MHz)	38.63	46.96	60.33	77.04	95.94	116.3	138.3	161.5	185.9

3. THE CONSTRUCTION OF THE DOUBLET FREQUENCY-BAND DEFLECTOR AND THE RESULTS OF MEASUREMENTS

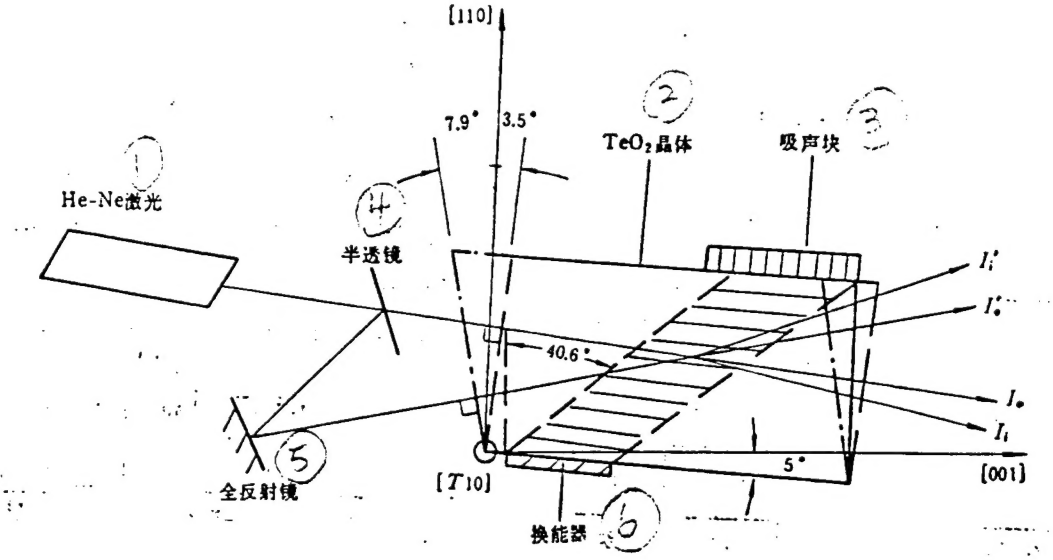

Fig. 2 The sketch of the doublet frequency-band TeO_2 sonic-optical deflector, actually taken from the realistic directional lines of the crystal itself; ... line stands for the direction taken by the crystal when the Dixon equation yields the positive solution; _._ line is for the direction of the crystal when the Dixon Equation yields the negative solution.

Key: (3) Sound speaker (4) half-transparent mirror
(5) Fully transparent mirror (6) transducer

From Table 3, one can see that a certain Θ_a angle corresponds to the 2 sets of incident angles and central frequencies. Thus by use of this phenomenon one can design a doublet frequency-band deflector. During the design it was found that the TeO_2 crystal could create very severe attenuation at the high end of the sound frequency of the "wave modified by truncation", and thus the high end of the frequencies of the deflector should not get too high, in general not to exceed 160 MHz. On the other hand, when the value of Θ_a is increased, the incident angle also increased, as to require a larger size for the crystal to accommodate large spreading directions, and thus we chose Θ_a to be 5°. At this time the corresponding f_o and Θ_i are respectively f_o = 61 MHz and f_o' = 116 MHz; Θ_i = 3.5° and Θ_i' = 7.9°. We utilized the flux-branching method, to split the laser beam into 2 fluxes, one of which was emitted along the sound wave propagation direction forming a 7.9° angle with respect to the [001] axis. The other flux was emitted in the direction reverse from the sound wave propagation, forming a 3.5° angle with respect to the [001] axis. For Θ_a = 5°, the wave-vector of the sound in the propagation direction and the energy propagation direction form a 40.6° angle. Fig.2 shows a sketch of the doublet frequency-band TeO_2 sonic-optical deflector. In the figure, the solid line shows the actual directions of the TeO_2 crystal, and the hollowed line shows the crystalline directions when the Dixon equation yields the positive solution, while the dotted line shows the crystalline directions when the Dixon equation yields the negative solution. In actuality, when the crystal was built, the incident surface was made perpendicular to the [001] axis, but at the time of testing, the incident beam fluxes formed angles of 3.5° and 7.9° with respect to the [001] axis. Thus here one finds that there has been some surface reflective losses.

In the TeO_2 deflector of doublet frequency-band, a X-cut $LiNbO_3$-transducer works in the 2 active band-widths. Since we are worrying about the high frequency attenuation of the "waves modified by truncation", by choosing the central frequency at 95 MHz, the results showed the high frequency efficiency was higher than that of low frequencies. Fig. 3 shows the results of measurements on the sound responding to the instrument frequencies. As it can be seen from the figure, the first set of 3 dB band-width was 40 - 80 MHz with the peak value efficiency reaching 90 %. The range of the 2 nd set of 3 dB active band-width was 80 - 140 MHz, with its peak value efficiency reaching 80 %. The difference in the diffraction efficiencies of these 2 sets is due to the fact that we let the X-cut $LiNbO_3$ transducer adjust the vibrational frequencies to reach some excessive value. After many repeated experiments, the appropriate vibrational frequency of the transducer could be chosen to allow the diffraction efficiencies of the 2 sets to be close onto each other.

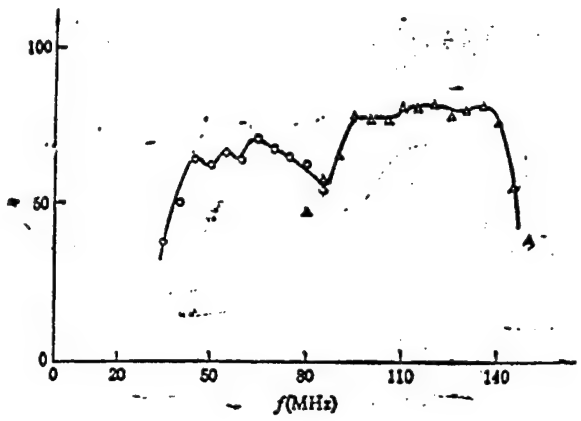

Fig. 3 Sonic response to the frequency of the TeO_2 sonic-optical deflector of doublet frequency-band

o stands for the positive solution of the Dixon equation

Δ stands for the negative solution of the Dixon equation

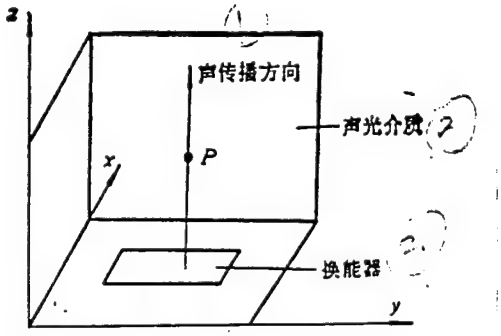

Fig. 4 Sketch of the sonic-optical device

Key: (1) sound propagation direction (2) sonic-optic medium (3) transducer

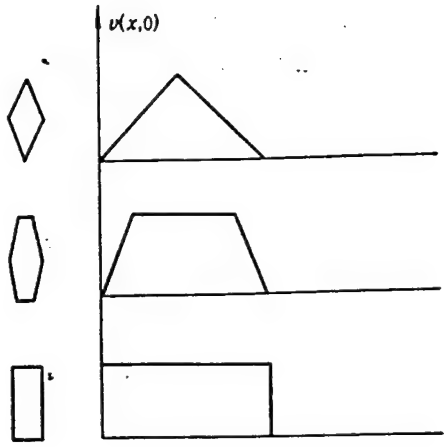

Fig. 5 Relationship between the shapes of the electric terminals and $v_{(x,0)}$

4. STRUCTURE OF THE SUPERSONIC TRANSDUCER

The sonic spreading of any sonic-optic device strongly affects the device in many of its applications. Especially, the sonic flux spread of the "wave modified by truncation" puts a limit on the apertures of any soni-optic device. Cook, et al. [7], suggested the choosing of appropriate electric terminal shapes so that it can generate the integral response of the diffraction beam and thus clearly it can improve the sonic field spread.

Fig. 4 is a sketch of a sonic-optic device. In the figure, the acoustic pressure p is determined by P(x,y,z). As the optic ray propagates along the y-axis, its diffraction is determined by the following equation:

$$V_{(x,z)} = k \int p(x,y,z)dy \tag{10}$$

Eqn.(10) expresses the integral response of the diffraction ray, where k is a constant. When z is zero, the acoustic field at the lower side of the transducer is determined by the shape of the electric terminal. When z is not zero, by going through a double Fourier transformation, one gets [8]

$$p(k_x,k_y,z) = \iint p(x,y,z)e^{-ik_x x}e^{-ik_y y}dxdy \tag{11}$$

where $k = 2\pi/\lambda$. At $k_y = 0$, one gets a single Fourier transformation, namely

$$p(k_x,z) = \int[\int p(x,y,z)dy]e^{-ik_x x}dx \tag{12}$$

In the above equation, the integrand is V(x,z). The acoustic pressure V(x,z) is determined by the shape of the transducer at z = 0. Consequently, as the distance z p away

from the transducer, the integral response can be found from the reverse transformation of $p(k_{x,o})\ \exp(ik_z z_o)$, namely

$$V_{(x,z_0)} = \int p(x,y,z_0)dy = \int e^{ik_z Z_0} p(k_x,0) e^{ik_x x} dk_x \tag{13}$$

Fig. 5 shows the V(x,0) functions for various shapes of the electric terminals. For various different sonic-optical interactions, one needs a multiplier coefficient for the sound wave-length (1-2b), where b is the quadratic coefficient [9] of the slower curve in the vicinity of a pure membrane axis. Now we can use the projection method to measure the photographs of acoustic fields (fig. 6) for the electric terminals of rectangular shape, rhombic shape and hexagonal shape.

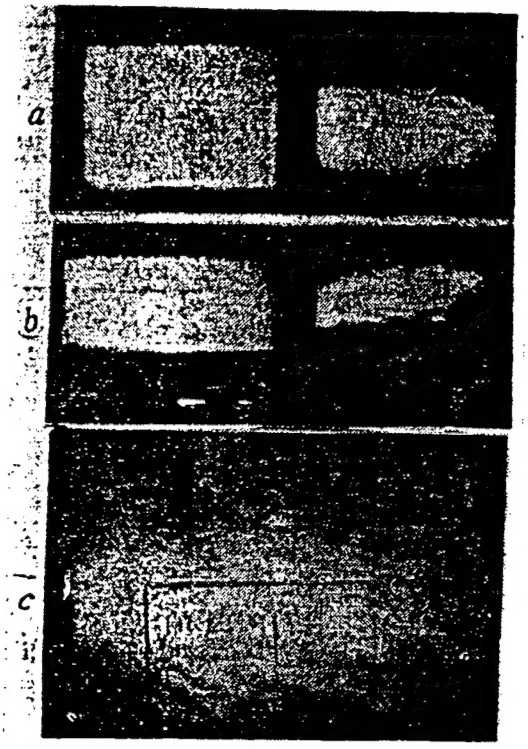

Fig. 6 The acoustic field distribution in the cross-section of a sonic-optic device

a. rhombic electric terminal; b. hexagonal electric terminal; c. rectangular electric terminal. In Fig. (a) and (b) the left side figures are the cross-sections of the TeO_2 crystal.

In Fig. (a) and (b) the left figures show the cross-sections of the TeO_2 crystal, while the right side figures show the acoustic field distributions. One can see from the figure that the rhombic shape electric terminal can improve the acoustic spreading.

5. CONCLUSION

In the actual application of the doublet frequency-band TeO_2 sonic-optical deflector, by arranging 2 sets of photoelectric diode tubes in sequence, splitting-and-transforming it to receive 2 frequency-bands of diffraction beams, one can broaden the band-width by 1 - 1.5 times, as compared to the case of using a single frequency-band deflector. Furthermore, this paper suggests that the rhombic shape of an electric terminal not only can be used in deflectors, but also in sonic-optic controller and multi-channel sonic-optic devices, in lowering the side-lobe level for the diffraction beams.

REFERENCE

[1] G. Arlt and H. Schweppe. : Solid State Commum., 6 (1968), 783.

[2] R. W. Dixon, IEEE J. Quantum Electron., QE-3 (1967), 85.

[3] E. G. H. Lean, C. F. Quate and H. T. Shaw, Appl. Phys. Lett. 10 (1967), 48.

[4] A. W. Warner, D. L. White and W. A. Bonner, J. Appl. Phys., 48 (1972), 4489.

[5] J. Yano and A. Watanabe, J. Appl. Phys., 45 (1974), 1243.

[6] Jiabin Shi, Principles of Sonic-Optic Instruments, Design and Application, Scientific Publishing Co., 1982.

[7] B. D. Cook, E. Cavanagh and H. O. Darby, IEEE Transactions on Sonics and Ultrasonics, SU-27-4 (1980), 674.

[8] Goodman, "Introduction to Fourier Optics" McGraw Hill, San Francisco, 1968.

[9] M. G. Cohen, J. Appl. Phys., 38-10 (1967), 1243.

DISTRIBUTION LIST

DISTRIBUTION DIRECT TO RECIPIENT

ORGANIZATION	MICROFICHE
B085 DIA/RTS-2FI	1
C509 BALLOC509 BALLISTIC RES LAB	1
C510 R&T LABS/AVEADCOM	1
C513 ARRADCOM	1
C535 AVRADCOM/TSARCOM	1
C539 TRASANA	1
Q592 FSTC	4
Q619 MSIC REDSTONE	1
Q008 NTIC	1
Q043 AFMIC-IS	1
E051 HQ USAF/INET	1
E404 AEDC/DOF	1
E408 AFWL	1
E410 AFDTC/IN	1
E429 SD/IND	1
P005 DOE/ISA/DDI	1
P050 CIA/OCR/ADD/SD	2
1051 AFIT/LDE	1
P090 NSA/CDB	1
2206 FSL	1

Microfiche Nbr: FTD94C000590
NAIC-ID(RS)T-0577-94